Asian Journal of Green Chemistry 4 (2020) 434-443

Asian Journal of Green Chemistry

Journal homepage: www.ajgreenchem.com

Short Cominucation

A green one-pot shortcut to light switching Tröger base analogs

Masoud Kazem-Rostami[a,*], Sadegh Faramarzi[b], Jeffrey L. Petersen[c]

[a] *Faculty of Science and Engineering, Macquarie University, North Ryde, NSW 2109, Australia*

[b] *Department of Biomedical Engineering, University of Minnesota, Minneapolis, MN 55455, USA*

[c] *Eugene Bennett Department of Chemistry, West Virginia University, Morgantown, WV 26506, USA*

ARTICLE INFORMATION

Received: 14 August 2019
Received in revised: 5 September 2019
Accepted: 14 September 2019
Available online: 31 January 2020

DOI: 10.33945/SAMI/AJGC.2020.4.7

KEYWORDS

Tröger base
Amine
Diazotization
Azo
Coupling reaction

ABSTRACT

Optimized desublimation of 2,4-diaminotoluene (4-methylbenzene-1,3-diamine) formed its ultrapure crystals. The collected crystals were analyzed by X-ray crystallography and then directly consumed in a condensation reaction with paraformaldehyde that resulted in the formation of Hünlich's base. The subsequent one-pot diazotization and coupling reactions produced a new bisazo analog of Tröger's base in the maximum possible compliance with the principles of green chemistry. The obtained bisazo product was found to be a durable and affordable building block suitable for use in the design of light-driven molecular machines.

Graphical Abstract

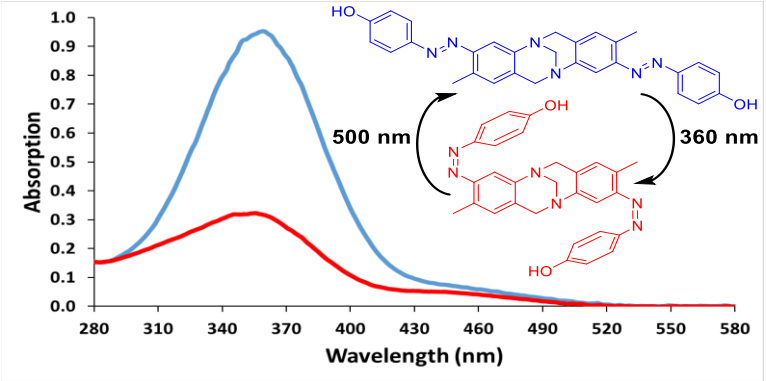

Corresponding author, email: masoud.kr@gmail.com (M. Kazem-Rostami).
Tel.: +612 98508275, Fax: +612 9850 8313.

Introduction

Phenylenediamines have been the staple of the production of high-performance synthetic materials, *e.g.,* aramid fabrics including nomex, kevlar, and twaron, despite being sensitive to air, light, and heat [1, 2]. Oxamniquine, moricizine, olanzapine [3], imatinib, quinoxalines [4], benzodiazepines [5], thiazoles [6], and benzimidazoles (*e.g.,* benomyl) [7–9] are a few examples of the bioactive materials derived from phenylenediamines. In particular, *m*-phenylenediamines have been utilized in the design of a variety of charge stabilizers [1], diazabicyclic cores [10], *m*-aramids, fluorescent tags (*e.g.,* ethidium salts), acridine [11], and azo dyes [12] including Bismarck brown Y [13].

Among the *meta*-analogs, 2,4-diaminotoluene is one of the most popular and fragile diamino building blocks that has been employed in the synthesis of imatinib (an anticancer medicine), acridine yellow G (a versatile dye), toluene diisocyanate (a reagent for the preparation of porous and flexible polyurethanes) [14], and Hünlich's base [15] (a diamino analog of Tröger's base).

Tröger base analogs have been utilized in the design of membranes [16], photoswitchable monomers [17], liquid crystal dopants [18, 19], fluorescent pH probes [20], lambda shape building blocks [21], molecular dual switches [22] and hinges [23]. This work introduces an efficient method for the purification of 2,4-diaminotoluene and a green one-pot synthetic route for its transformation to a light-responsive analog of Tröger's base.

Experimental

Materials and methods

Eppendorf kinetic-bio and thermo scientific nicolet iS5/10 performed the UV-vis and ATR-IR spectrophotometries. Bruker DRX 400 and agilent quadrupole-6130 recorded the NMR and HPLC-coupled mass spectra. Vario el-elementar analyzer performed the elemental analysis. DSC 2010 instrument (TA-instruments, USA) performed the differential scanning calorimetry using the standard aluminum DSC pan and lid (*C*-type) under a flowing nitrogen atmosphere (0.05 L/min^{-1}, N_2 99%). Merck DC-kieselgel 60-F_{254} aluminum plates and spectroline ENF-260 C/FE UV lamps [230 V, 0.17 A, 50 Hz; 256/365 nm] were employed in TLC. The 365 nm band was also used for the illumination of capped quartz cuvettes loaded with the solution of the bisazo product for 5 min. The dark-incubated and illuminated samples represented the fully relaxed (*trans-trans*) photoisomer and photostationary state (mainly containing *cis-cis* and trace amounts of *cis-trans* photoisomers). Sigma-aldrich and Cambridge isotope laboratories Inc. supplied the chemicals and NMR solvents, respectively.

Sublimation/desublimation of 2,4-diaminotoluene

Brownish black pellets of 2,4-diaminotoluene (3.0 g, approx. 25 mmol) were placed in a 250 mL sublimation apparatus immersed in a sand bath. The sublimation chamber was heated under reduced pressure in the absence of light (35±10 mbar, 140±2 °C) while its cold-finger condenser was cooled by the constant circulation of water (19±2 °C, 2 L/min^{-1}). Once the needle looking white crystals stopped growing, the chamber was sealed, the vacuum pump and heater were turned off, and the apparatus gradually cooled down to room temperature in the dark. Afterward, the chamber was filled with nitrogen and the deposited white crystals were collected. At the bottom of the sublimation chamber a tar-like residue (0.42 g, 14 wt.%) solidified at room temperature. This residue showed no trace of 2,4-diaminotoluene in the proton NMR analysis and hence was crushed by spatula and discarded. Yield 2.34 g (19.5 mmol, 78 wt.%, approx. crystal length: 5–40 mm); R_f = 0.4 (silica gel; MeOH/DCM = 2% v/v). ^{1}H NMR (400 MHz, DMSO-*d*$_6$): δ 6.55 (d, *J* = 7.8, 1H, CH), 5.88 (d, *J* = 2.2, 1H, CH), 5.75-5.77 (dd, *J* = 7.8, *J* = 2.2, 1H, CH), 4.43 (d, *J* = 5.7, 4H, NH), 1.89 (s, 3H, CH_3). MS (ESI+; CAN-H_2O = 90% v/v): *m/z* $[M + H]^+$ calcd for $[C_7H_{11}N_2]^+$: 123.09, found 123.1. Anal. Calcd for $C_7H_{10}N_2$: C, 68.82; H, 8.25; N, 22.93. Found: C, 68.86; H, 8.21; N, 22.87. CCDC deposition number: 1937265.

One-pot synthesis of 4,4'-((1E,1'E)-(2,8-dimethyl-6H,12H-5,11-methanodibenzo[b,f][1,5] diazocine-3,9-diyl)bis(diazene-2,1-diyl))diphenol

Trögeration step: 2,4-diaminotoluene (3.6 g, 30 mmol) was placed in a 100 mL round bottom flask and topped off with degassed aqueous HCl solution (12%, 80 mL, 0 °C). Once the contents became homogeneous, paraformaldehyde (1.3 g, 45 mmol) was added. The flask was then capped and wrapped in aluminum foil and its contents stirred for 24 h at room temperature. In parallel experiments, the reaction profile was monitored by HPLC-MS. Once the improvements and completion of the reaction were confirmed by HPLC-MS, one of each batches was worked-up to evaluate the Hünlich base obtained as an off-white solid 2.4 g (57%), R_f = 0.5 (silica gel; MeOH/DCM = 10% v/v). ATR-IR (ν_{max}/ cm^{-1}): 3405, 3337, 3235, 2888, 1619, 1498, 914, and 870. ^{1}H NMR (400 MHz, DMSO-*d*$_6$): δ 6.42 (s, 2H, CH), 6.28 (s, 2H, CH), 4.55 (b, 4H, NH), 4.33-4.37 (d, *J* = 16.2 Hz, 2H, C6-Hb/C12-Hb), 4.02 (s, 2H, -NCH_2N-), 3.76-3.80 (d, *J* = 16.2 Hz, 2H, C6-Ha/C12-Ha), 1.91 (s, 6H, 2CH_3). MS (ESI+; EtOH): *m/z* $[M + H]^+$ calcd for $[C_{17}H_{21}N_4]^+$: 281.17, found 281.1. Anal. Calcd for $C_{17}H_{20}N_4$: C, 72.83; H, 7.19; N, 19.98. Found: C, 72.98; H, 7.31; N, 19.86.

Diazotization and coupling steps

The acidic solution of Hünlich's base was cooled down to -5 °C, $NaNO_2$ (2.1 g, 30 mmol) was slowly added and stirred for 30 min. Afterwards, added phenol (2.8 g, 30 mmol) and raised the pH to 7 by the gradual addition of Na_2CO_3 (1.5-2 g). The mixture was stirred for 4 h and then filtered. The

collected orange particles were rinsed with water, desiccated, and dissolved in warm absolute ethanol, filtered and recrystallized twice. The collected amorphous crystals were crushed and dried under reduced pressure to obtain the final bisazo product. Yellowish orange powder, yield 4.6 g (62%), R_f = 0.4 (silica gel; EtOAc/*n*-Hexane = 50% v/v). ATR-IR (ν_{max}/ cm^{-1}): 2952, 1586, 1482, 1236, 1134, 1079 and 837. ^{1}H NMR (400 MHz, DMSO-d_6): δ 10.25 (s, 2H, OH), 7.79 (d, J = 8.1 Hz, 4H, CB-H), 7.28 (s, 2H, C4-H/C10-H), 6.95 (s, 2H, C1-H/C7-H), 6.94 (d, J = 8.1 Hz, 4H, CA-H), 4.62-4.66 (d, J = 16.2 Hz, 2H, C6-Hb/C12-Hb), 4.26 (s, 2H, C13-H or -NCH_2N-), 4.14-4.18 (d, J = 16.2 Hz, 2H, C6-Ha/C12-Ha), 2.48 (s, 6H, C2-CH_3/C8-CH_3). ^{13}C NMR (100 MHz, DMSO-d_6): δ 160.7, 149.1, 146.5, 145.6, 132.0, 130.8, 129.3, 124.8, 115.9, 110.4, 66.2, 58.4, 16.5. MS (ESI+; EtOH): *m/z* $[M + H]^+$ calcd for $[C_{29}H_{27}N_6O_2]^+$: 491.22, found 491.2. MS (ESI–; EtOH): *m/z* $[M-H]^-$ calcd for $[C_{29}H_{25}N_6O_2]^-$: 489.20, found 489.2. Anal. Calcd for $C_{29}H_{26}N_6O_2$: C, 71.00; H, 5.34; N, 17.13. Found: C, 69.85; H, 5.46; N, 16.97.

Results and Discussion

The sensitive nature of 2,4-diaminotoluene leads to its degradation, indicated from its gradual change of color from white to brownish black. In the synthetic processes, this phenomenon coincides with the generation of more unwanted impurities that are difficult to remove from the sensitive (*e.g.*, Hünlich's base) or polymeric (*e.g.*, *m*-aramids) products. Therefore, in this work, these impurities had been eliminated prior to the initial use of 2,4-diaminotoluene in the synthesis of Hünlich's base. Although such an initial purification step can be seemingly more convenient and cost-effective than the purification of Hünlich's base, various methods of crystallization in solution and liquid chromatography practically fail to readily purify 2,4-diaminotoluene due to its rapid degradation. Therefore, a vacuum-assisted sublimation/desublimation method was optimized providing a highly pure crystalline form of 2,4-diaminotoluene at multigram scale (Figure 1). The optimized desublimation, unlike chromatography and solvothermal crystallization, does not require any organic solvent and takes less time. The suggested temperature gradient desublimation in vacuo resulted in the significant growth of crystals and recovery percentages (78-83%). The X-ray crystallographic analysis of the obtained crystals revealed the existing intermolecular hydrogen bonding interactions and the unit system (Figure 1). The red dashed line in Figure 1 (bottom right) shows the orientation of a weak intermolecular hydrogen bonding interaction between atom N1 and atom H2A of a symmetry-related molecule. The results of quantum mechanical calculations, with density functional theory (DFT) and B3LYP/6-31++G(d,P) basis set (Figure 1, top in red) [24], and the experimental crystal structure studies (Figure 1, top in blue) of 2,4-diaminotoluene were then compared. The root mean square deviation (RMSD) between the two structures was 0.125 Å, proving that the structures match.

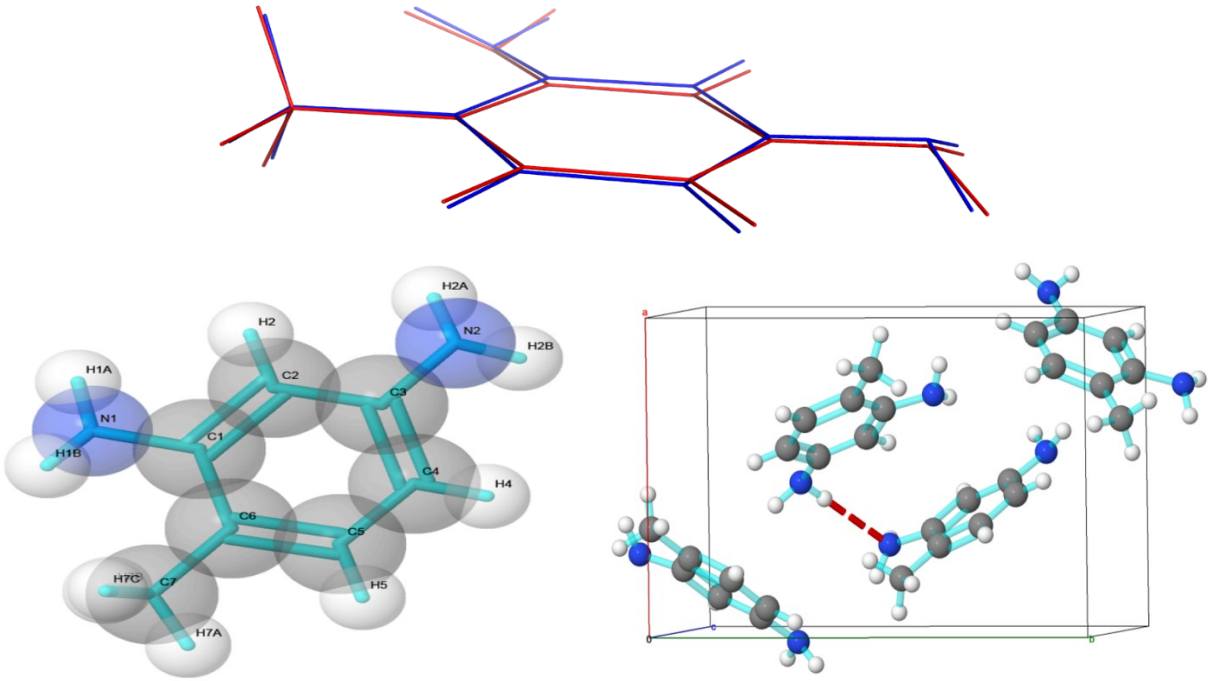

Figure 1. Superimposed wireframe structures of 2,4-diaminotoluene obtained from X-ray crystallographic analysis (top in blue) and quantum mechanical calculations with Gaussian 09 package [25] (top in red). Translucent ball & stick presentation of the molecular structure of 2,4-diaminotoluene ($C_7H_{10}N_2$) with the atom labeling scheme (bottom left) and perspective opaque view of a unit cell packing diagram viewed along the *c*-axis, for the orthorhombic crystal lattice of 2,4-diaminotoluene (bottom right); the thermal ellipsoids are scaled to enclose 50 and 20% probability, respectively

The obtained crystals were directly used in a condensation reaction between 2,4-diaminotoluene and paraformaldehyde for the synthesis of Hünlich's base (Scheme 1). It is known that the *ortho* amine groups (Scheme 1, indicated in red) neither interfere with the trögeration [23] nor form side-products [15]. Scheme 1 displays the stepwise mechanism of the acid-induced condensation reaction, producing Hünlich's base as the major product, on the basis of Wagner's rationale [26] considering the role of the unreacted *ortho* amine groups in the activation and closure of phenyl and diazocine rings, respectively. Although the condensation reaction requires a rather strongly acidic medium, the conjugate base has almost no role to play. Therefore, HCl was substituted for H_2SO_4 to improve the atom economy and avoiding any buffer resistance during the work-up. Paraformaldehyde was also substituted for formaldehyde as a safer alternative, making the reaction more controlled and cleaner. The hydrolysis of paraformaldehyde occurs in both alkaline and acidic media; however, it is faster at low pH and high temperature [27]. The presence of the mineral acid in the trögeration reaction is inevitable owing to its catalytic role. Therefore, the temperature was decreased to decelerate the

hydrolysis of paraformaldehyde and its reaction with 2,4-diaminotoluene, minimizing the chances for side-reactions.

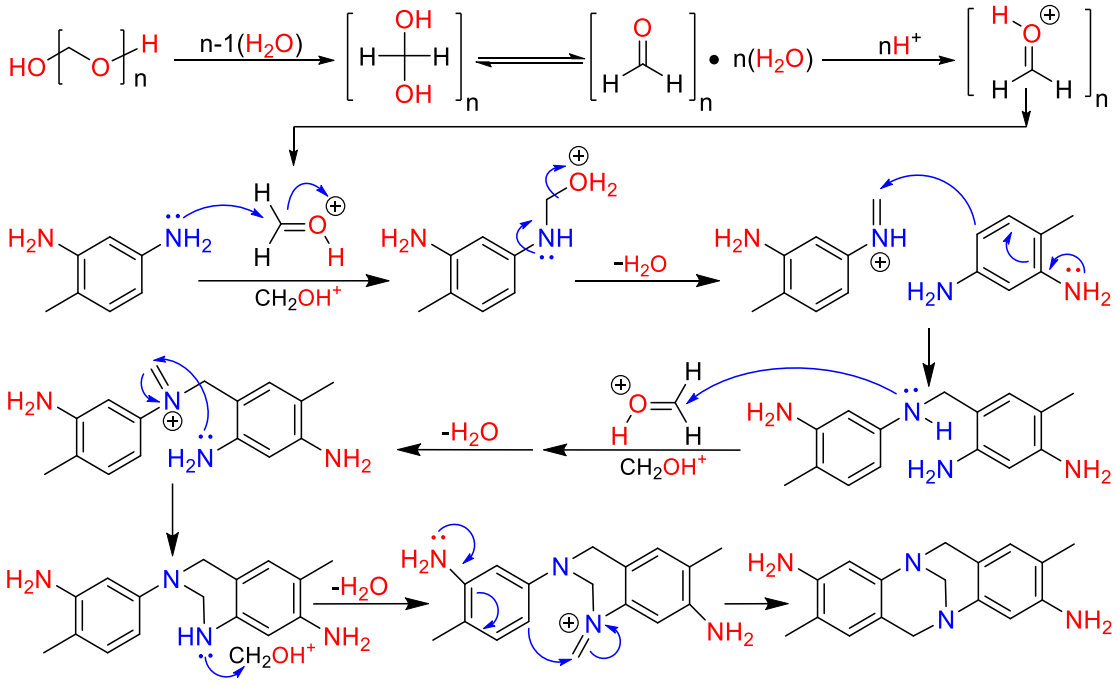

Scheme 1. Simultaneous acid-catalyzed hydrolysis of paraformaldehyde and its condensation with 2,4-diaminotoluene resulting in Hünlich's base

The use of ultrapure 2,4-diaminotoluene along with mild reagents significantly enhanced the reaction profile, improved the yield, and resulted in a clean solution of Hünlich base hydrochloride whose formation was monitored by HPLC-MS. This solution met the acidic condition required for the diazotization reaction and hence was directly used without work-up. This shortcut not only saved time, energy, solvent, and reagent but also prevented the exposure of Hünlich's base to light, heat, and air. Subsequently, the diazotization and coupling reactions were initiated by the addition of sodium nitrite and phenol that produced a new bisazo carrying analog of Tröger's base (Scheme 2). Unlike the previous reports [17, 23], in this work Hünlich base was prepared and used in one-pot to reduce the number and amount of consumed reagents (Scheme 2). As a result, the use of organic solvents, corrosive and toxic solutions of ammonia and formaldehyde has been avoided. Furthermore, the amount of the required acids and bases have been reduced to a half, and the total volume of water used as solvent to almost a third (from 285 to 115 mL per gram of bisazo product).

The UV/vis absorption spectra of the obtained bisazo compound indicated its response to photonic stimulant of 365 nm. The *trans-trans* (*i.e.,* unswitched, *EE* or relaxed) and *cis-cis* (*i.e.,* double-switched, *ZZ* or photoexcited) were the major photoisomers existing in the dark-incubated solution

(Figure 2, shown in blue) and the illuminated solution that had reached a photostationary state (Figure 2, shown in red), respectively.

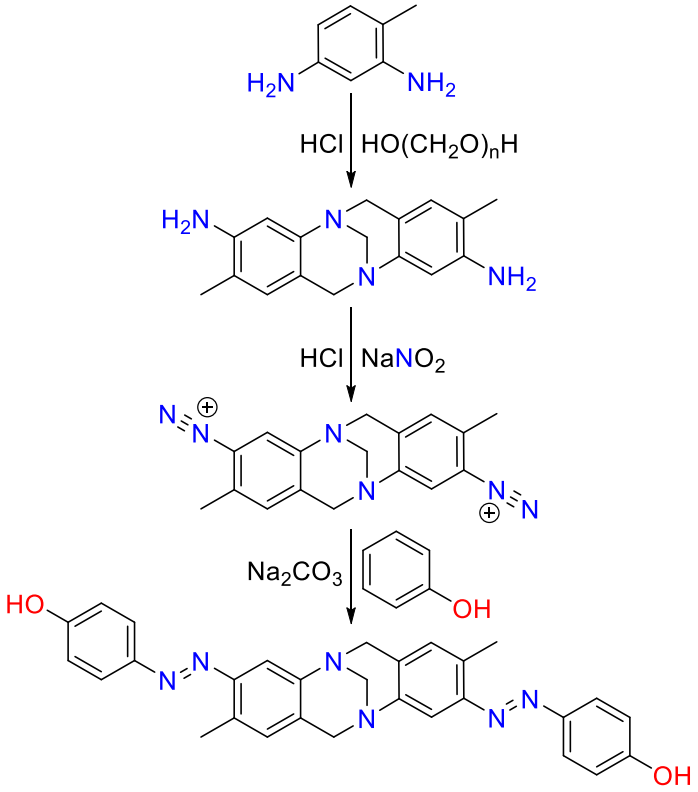

Scheme 2. One-pot synthesis of a bisazo derivative of Hünlich base in aqueous media

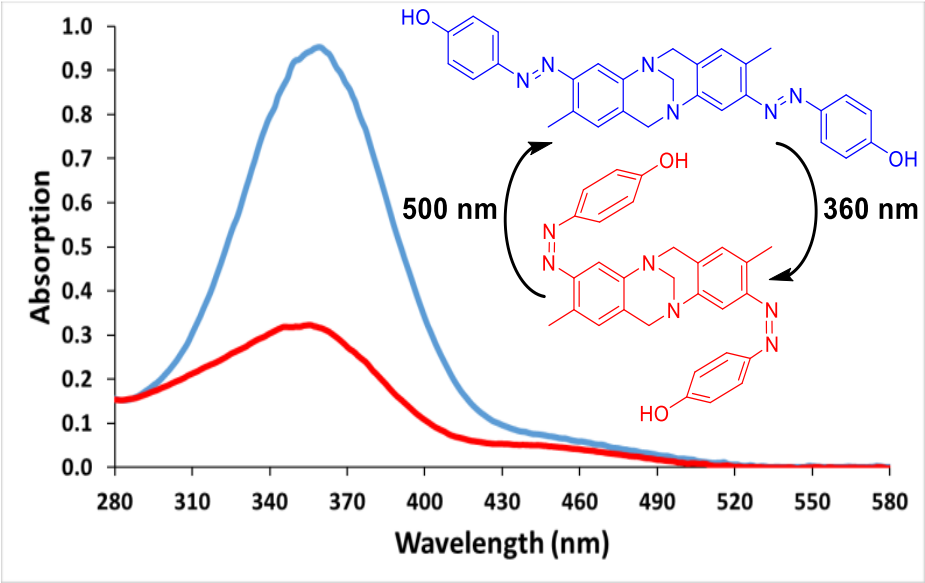

Figure 2. Overlaid UV/vis absorption spectra of dark-incubated (blue) and illuminated (red) solutions

Conclusions

In this work, toxic reagents were substituted for safer and cleaner alternatives. These included the use of sodium carbonate and paraformaldehyde instead of ammonia and formaldehyde. Dilute hydrochloric acid was also substituted for concentrated sulfuric acid to improve the atom economy and avoid buffer resistance during the work-up. The acid solution was degassed by ultrasound prior to use to reduce the presence of oxygen and the occurrence of side reactions. The neutralization of the acid was postponed to the final coupling step and hence the amount of applied acid and base was less than a half of those consumed in the previous works. The postponed neutralization of hydrochloric acid with sodium carbonate produced sodium chloride. This facilitated the precipitation of the final product and its collection with filtration instead of extraction with solvents. In addition, sodium chloride is safer than ammonium salts to dispose of it properly. The use of paraformaldehyde instead of formaldehyde at low temperature improved the trögeration yield. These enhancements and the mild one-pot procedure along with the initial elimination of the contaminants from the starting diamino compound improved the yield for both Hünlich's base (from 35 to 57%) and its bisazo derivative (28 to 62%). The desired bisazo product was obtained without the use of organic solvents and toxic reagents. The efficacy of the methods was improved, and the wastes were reduced both in volume and level of toxicity in order to reach the maximum possible compliance with the principles of green chemistry. Last but not least, the final bisazo product reversibly switched by light and remained stable, after prolonged UV exposure (6 h, 365 nm, 4 W) and at high temperature (<230 °C, tested by DSC under N_2), entitling it as a durable and affordable building block for the design of molecular machines.

Disclosure Statement

No potential conflict of interest was reported by the authors.

Supporting Information

Additional supporting information related to this article can be found, in the online version, at DOI: 10.33945/SAMI/AJGC.xxxx.x.x

Orcid

Masoud Kazem-Rostami 0000-0003-4821-5820

Sadegh Faramarzi 0000-0002-9739-9286

Jeffrey L. Petersen 0000-0001-8681-853X

Notes

CCDC 1937265 contain crystallographic data for this work; These data can be obtained free of charge *via* www.ccdc.cam.ac.uk (or from the Cambridge Crystallographic Data Centre, 12, Union Road, Cambridge CB2 1EZ, UK; Fax: +441223 336033). Supplementary information containing the chemical structures, copies of NMR, UV/vis, MS, ATR-IR spectra, DSC curves and HPLC-MS chromatograms is available online at www.ajgreenchem.com. The financial aid of the Australian Government (Research Training Program Scholarship: IPRS2014-004) and Macquarie University (HDR43010477 and PGRF2016-R2-1672525) are gratefully acknowledged.

References

[1]. Gessner T., Mayer U. *Triarylmethane and Diarylmethane Dyes*. In *Ullmann's Encyclopedia of Industrial Chemistry*; Wiley-VCH Verlag GmbH & Co. KGaA: Germany, 2000; p 425

[2]. Smiley R.A. *Phenylene- and Toluenediamines*. In *Ullmann's Encyclopedia of Industrial Chemistry*; Wiley-VCH Verlag GmbH & Co. KGaA: Germany, 2000; p 617

[3]. Madhav N.V.S., Singh B. *Asian J. Nanosci. Mater.,* 2019, **2**:314

[4]. Mirjalili B.B.F., Dehghani Tafti M. *Sci. Iran.,* 2017, **24**:3014

[5]. Goswami S., Hazra A., Jana S. *J. Heterocycl. Chem.,* 2009, **46**:861

[6]. de Andrade V.S.C., de Mattos M.C.S. *Synthesis,* 2018, **50**:4867

[7]. Rezaee Nezhad E., Tahmasebi R. *Asian. J. Green Chem.,* 2019, **3**:34

[8]. Khazaei A., Zolfigol M.A., Moosavi-Zare A.R., Zare A., Ghaemi E., Khakyzadeh V., Asgari Z., Hasaninejad A. *Sci. Iran.,* 2011, **18**:1365

[9]. Wang Z., Song T., Yang Y. *Synlett,* 2019, **30**:319

[10]. Gall' A.A., Sil'nikov V.N., Shishkin G.V. *Chem. Heterocycl. Compound.,* 1988, **24**:682

[11]. Zhang W.T., Chen D.S., Li C., Wang X.S. *Synthesis,* 2015, **47**:562

[12]. Khazaei A., Kazem-Rostami M., Zare A., Moosavi-Zare A.R., Sadeghpour M., Afkhami A. *J. Appl. Polym. Sci.,* 2013, **129**:3439

[13]. Heydari S., Habibi D. *Polyhedron,* 2018, **154**:138

[14]. Zhang X., Li S., Zhu X., Jiang X., Kong X.Z. *React. Funct. Polym.,* 2018, **133**:143

[15]. Rigol S., Beyer L., Hennig L., Sieler J., Giannis A. *Org. Lett.,* 2013, **15**:1418

[16]. Patel H.A., Selberg J., Salah D., Chen H., Liao Y., Mohan Nalluri S.K., Farha O.K., Snurr R.Q., Rolandi M., Stoddart J.F. *ACS Appl. Mater. Interfaces,* 2018, **10**:25303

[17]. Kazem-Rostami M. *Synthesis,* 2017, **49**:1214

[18]. Kazem-Rostami M. *New J. Chem.,* 2019, **43**:7751

[19]. Kazem-Rostami M. *J. Therm. Anal. Calorim.,* 2019, https://doi.org/10.1007/s10973-019-08884-4

[20]. Zhuge X., Liu R., Li J., Zhang J., Li Y., Yuan C. *Dyes Pigm.,* 2019, **171**:107678

[21]. Kazem-Rostami M. *Synlett,* 2017, **28**:1641

[22]. Kazem-Rostami M., Akhmedov N.G., Faramarzi S. *J. Mol. Struct.,* 2019, **1178**:538

[23]. Kazem-Rostami M., Moghanian A. *Org. Chem. Front.,* 2017, **4**:224

[24]. Parr R.G. *Density Functional Theory of Atoms and Molecules*. In Horizons of Quantum Chemistry; Springer: Netherlands, 1980; p 5-15

[25]. Frisch M.J., Trucks G.W., Schlegel H.B., Scuseria G.E., Robb M.A., Cheeseman J.R., Scalmani G., Barone V., Petersson G.A., Nakatsuji H., Li X., Caricato M., Marenich A.V., Bloino J., Janesko B.G., Gomperts R., Mennucci B., Hratchian H.P., Ortiz J.V., Izmaylov A.F., Sonnenberg J.L., Williams-Young D., Ding F., Lipparini F., Egidi F., Goings J., Peng B., Petrone A., Henderson T., Ranasinghe D., Zakrzewski V.G., Gao J., Rega N., Zheng G., Liang W., Hada M., Ehara M., Toyota K., Fukuda R., Hasegawa J., Ishida M., Nakajima T., Honda Y., Kitao O., Nakai H., Vreven T., Throssell K., Montgomery J.A., Jr. Peralta J.E., Ogliaro F., Bearpark M.J., Heyd J.J., Brothers E.N., Kudin K.N., Staroverov V.N., Keith T.A., Kobayashi R., Normand J., Raghavachari K., Rendell A.P., Burant J.C., Iyengar S.S., Tomasi J., Cossi M., Millam J.M., Klene M., Adamo C., Cammi R., Ochterski J.W., Martin R.L., Morokuma K., Farkas O., Foresman J.B., Fox D.J., Gaussian 16, Wallingford: USA, 2016

[26]. Wagner E.C. *J. Org. Chem.,* 1954, **19**:1862

[27]. Rossmoore H.W., Sondossi M. Applications and Mode of Action of Formaldehyde Condensate Biocides. In *Adv. Appl. Microbiol.*; Academic Press: USA, 1988; p 223

[28]. Chen J., Leung F.K., Stuart M.C.A., Kajitani T., Fukushima T., van der Giessen E., Feringa B.L. *Nat. Chem.,* 2017, **10**:132

[29]. Stoddart J.F. *Angew. Chem. Int. Ed.,* 2017, **56**:11094

How to cite this manuscript: Masoud Kazem-Rostami*, Sadegh Faramarzi, Jeffrey L. Petersen. A green one-pot shortcut to light switching Tröger base analogs. *Asian Journal of Green Chemistry*, 4(4) 2020, 434-443. DOI: 10.33945/SAMI/AJGC.2020.4.7